ORIGINAL ARTICLE

Reproductive Medicine and Biology | Open Access | **WILEY**

Aberrant expression of histone deacetylase 8 in endometriosis and its potential as a therapeutic target

Hanxi Zheng[1] | Xishi Liu[1,2] | Sun-Wei Guo[2,3]

[1]Department of Gynecology, Shanghai Obstetrics and Gynecology Hospital, Fudan University, Shanghai, China

[2]Shanghai Key Laboratory of Female Reproductive Endocrine-Related Diseases, Fudan University, Shanghai, China

[3]Research Institute, Shanghai Obstetrics and Gynecology Hospital, Fudan University, Shanghai, China

Correspondence
Sun-Wei Guo, Research Institute, Shanghai Obstetrics and Gynecology Hospital, Fudan University, Shanghai 200011, China.
Email: hoxa10@outlook.com

Present address
Hanxi Zheng, Center for Human Reproduction and Genetics, Affiliated Suzhou Hospital of Nanjing Medical University, Suzhou Municipal Hospital, Gusu School, Nanjing Medical University, Suzhou, China

Abstract

Purpose: To screen Zn^{2+}-dependent histone deacetylase (HDAC) 1-11 in endometriotic cells and then evaluated the HDACs identified from the screening in ovarian endometrioma (OE) and deep endometriotic (DE) lesions, and to evaluate the therapeutic potential of HDAC8 inhibition in mice.

Methods: Quantification of gene and protein expression levels of HDAC1-11 in endometriotic cells stimulated by TGF-β1, and immunohistochemistry analysis of Class I HDACs and HDAC6 in OE/DE lesion samples. The therapeutic potential of HDAC8 inhibition was evaluated by a mouse model of deep endometriosis.

Results: The screening identified Class I HDACs and HDAC6 as targets of interest. Immunohistochemistry analysis found a significant elevation in HDAC8 immunostaining in both OE and DE lesions, which was corroborated by gene and protein expression quantification. For other Class I HDACs and HDAC6, their lesional expression was more subtle and nuanced. HDAC1 and HDAC6 staining was significantly elevated in DE lesions while HDAC2 and HDAC3 staining was reduced in DE lesions. Treatment of mice with induced deep endometriosis with an HDAC8 inhibitor resulted in significantly longer hotplate latency, a reduction of lesion weight by nearly two-thirds, and significantly reduced lesional fibrosis.

Conclusions: These findings highlight the progression-dependent nature of specific HDAC aberrations in endometriosis, and demonstrate, for the first titme, the therapeutic potential of suppressing HDAC8.

KEYWORDS
endometriosis, fibrosis, histone deacetylase 8, progression, therapeutic

1 | INTRODUCTION

It has been nearly two decades since the first report of epigenetic aberration in endometriosis and, as such, the proposal that endometriosis may be an epigenetic disease.[1] Since then, many other epigenetic aberrations in endometriosis as well as in adenomyosis have been reported.[2–7] Moreover, it becomes evident that many genes/proteins involved in epigenetic modifications, such as histone deacetylases (HDACs),[8,9] DNA methyltransferases (DNMTs),[10,11] and various histone modifiers,[12–17] are also aberrantly expressed

---

in ectopic endometrium. Following on the heels of the discovery of various epigenetic aberrations, pharmacological options have been sought to rectify these anomalies. In particular, HDAC inhibitors (HDACIs) have been demonstrated in preclinical studies by many groups to be a promising therapeutic.[5,18–31] This led to the encouraging reports of the use of valproic acid (VPA), an HDAC inhibitor, in treating adenomyosis.[32,33] Unfortunately, however, there has been no independent validation so far.

Given the strong undercurrent, which surfaced only recently, against hormonal drugs among patients with endometriosis[34] and the stagnation in developing non-hormonal drugs for endometriosis/adenomyosis,[35,36] the apparent lack of continuation of this line of research is somewhat unsettling. Naturally, the long expired patent of VPA certainly provides little financial incentive to any pharmaceutical company interested in sponsoring a trial to further test this drug.

Granted, VPA is a Category D drug and is contraindicated for those who are pregnant or plan to. However, it has a fast clearance rate, with a half-life ranging from 5 to 20h. In addition to its desirable antiproliferative and anti-inflammatory propensity and its capability to reactivate silenced PR-B,[5] VPA has been shown to suppress uterine contraction[24,37] and contain fibrosis.[38–42] Uterine hyperactivity is a well-recognized contributor to dysmenorrhea,[43] and fibrosis has emerged fairly recently as one important hallmark of endometriosis.[44,45] VPA also has been reported to alleviate neuropathic pain.[46,47] These desirable properties make VPA a very promising therapeutic for treating endometriosis and adenomyosis.

Nonetheless, VPA is by no means the best drug in its class. More importantly, further research is needed to identify exactly which HDACs are actively involved in lesional progression and fibrogenesis since histone acetylation is an integral part of epigenetic modification and is synergistically regulated by histone acetyltransferase (HAT) and HDAC. To date, 18 human HDACs have been identified, which are grouped into four classes based on their sequence homology and domain organization: Class I (HDAC1-3, and 8), Class II (HDAC4-7, 9 and 10), Class III (SIRT1-7) and Class IV (HDAC11).[48] Classes I, II, and IV HDACs are Zn^{2+}-dependent and are often called classical HDACs.[48] In contrast, Class III HDACs use NAD^+ as a cofactor for catalytic activity. Of note, existing HDACIs do not directly affect the activity and function of Sirtuins,[49] and VPA is a Classes I and II HDAC inhibitor.[50,51] In other words, VPA inhibits more than one HDAC yet it is unclear exactly which HDACs are actively involved in lesional progression.

In endometriosis, the precise role of HDACs is still poorly understood. Even for the most studied Class I HDACs, there are conflicting reports of their aberration in endometriosis. For example, while both HDAC1 and HDAC2 are reported to be overexpressed in endometriosis,[52] a later report only found HDAC1 overexpression.[8] Apparently, in order to pave the way for the use of HDACIs as therapeutics, it is necessary to delineate the roles of each individual HDACs in endometriosis.

Given the importance of fibrogenesis in endometriosis,[44,45] and in view of the roles of HDACs in different fibrotic disorders, such as heart,[53] lung,[39] liver,[54,55] and renal[56] fibrosis, we believe that it

is necessary to further investigate HDACs in endometriosis. This is especially timely since many studies have shown that various HDACs, such as HDAC1,[57] HDAC2,[58–60] HDAC3,[61] HDAC4,[62,63] HDAC6,[64,65] HDAC7,[66] and HDAC8,[67] play important roles in epithelial-mesenchymal transition (EMT), fibroblast to myofibroblast transdifferentiation (FMT), and mesothelial to mesenchymal transition (MMT)—and these processes have been documented to drive the progression of endometriosis.[45,68] Since different HDAC subtypes appear to accelerate or decelerate fibrogenesis in different diseases or in a redundancy manner, and HDACIs have therapeutic potential in fibrosis-associated diseases,[69] identification of specific HDAC subtypes that drive EMT, FMT, and fibrogenesis becomes a pressing prerequisite for drug development for endometriosis.

In this study, we tasked ourselves to screen Classes I, II, and IV HDACs in endometriotic epithelial and stromal cells that are stimulated by the archetypical profibrotic cytokine, transforming growth factor β1 (TGF-β1), that is known to induce EMT, FMT, smooth muscle metaplasia (SMM) and MMT in endometriosis.[68,70,71] We then evaluated the HDACs identified from the screening in ovarian endometrioma (OE) and deep endometriotic (DE) lesions. Based on the results thereof, we conducted a serial mouse experiment and evaluated the lesional staining of Class I Hdacs and Hdac6, and evaluated the effect of Hdac8 activation and suppression on lesional development—but this part is reported elsewhere.[72] We also evaluated the therapeutic effect of suppression of HDAC8 in mice with induced deep endometriosis.

2 | METHODS AND MATERIALS

2.1 | Human tissue samples

After written informed consent, two sets of endometriotic tissue samples were obtained. The first set consisted of 13 patients with histologically confirmed OE and 11 patients without (Table S1). The tissue samples were used to derive primary endometriotic/endometrial stromal cells (see below). The second set consisted of 58 premenopausal women with laparoscopically and histologically diagnosed endometriosis without other gynecological diseases (except adenomyosis and uterine fibroids), who received no hormonal treatment at least 3months before the surgery. These patients were recruited consecutively from December 2018 to May 2020 and received operations in the OB/GYN Hospital of Fudan University. Among these patients, 38 of them were operated on for OE, and the remaining 20 for DE. As controls, endometrial tissue samples were obtained after written informed consent from 24 cycling women, roughly age- and menstrual phase-matched with patients in the OE or DE group, who underwent surgery for cervical squamous intraepithelial lesion but were free of endometriosis, adenomyosis, and uterine abnormalities.

For all recruited participants, information on the phase of the menstrual cycle, the severity of dysmenorrhea (on a verbal descriptor scale, namely, none, mild, moderate, and severe), gravidity, parity,

revised American Society for Reproductive Medicine Classification of Endometriosis (rASRM) stage (for endometriosis patients only) and co-occurrence of adenomyosis or uterine fibroids were retrieved. None of the recruited participants were smokers or heavy drinkers. This study was approved by the Ethics Review Committee of Shanghai Obstetrics and Gynecology Hospital, Fudan University (on file). The characteristics of the recruited participants are listed in Table 1.

2.2 | Cells and reagents

The endometriotic epithelial cell line (11Z), established by Professor Anna Strazinski-Powitz,[73] was a gift kindly provided by Dr. Jung-Hye Choi of Kyung Hee University, Seoul, Republic of Korea. Cells were cultured in RPMI 1640 medium (Gibco, Grand Island, NY, USA) supplemented with 5% fetal bovine serum (FBS) (Gibco), 100 IU/mL penicillin G, 100 mg/mL streptomycin, and 2.5 µg/mL Amphotericin B. Human primary endometriotic stromal cells derived from ovarian endometrioma (hESCs) were cultured as reported previously.[70] Normal human endometrial stromal cells (NESCs) were cultured using the same protocol. Briefly, both normal and ectopic endometrial tissues were washed with phosphate-buffered saline (PBS) and minced into pieces as small as possible. The minced tissues were then enzymatic digested with 0.2% collagenase IV (Sigma, St. Louis, MO, USA) and incubated in a shaking bed for 1.5 h at 37°C. The cell components were separated by filtrated successively through a 76-mm and then a 37-mm nylon mesh (Falcon, Corning, NY, USA). The filtrated cells were centrifuged and resuspended in Dulbecco's modified Eagle's medium/Ham's F-12 medium (DMEM/F-12, Hyclone, South Logan, UT, USA) supplemented with 10% FBS, 100 IU/mL penicillin, 100 mg/mL streptomycin, and 2.5 µg/mL Amphotericin B. Cell were seeded into 25-cm^2 cell culture flasks and incubated in a humidified atmosphere of 5% CO_2 at 37°C. Their purity was verified by whole-cell immunochemical staining as reported previously.[70] All cells were cultured in a humidified incubator at 37°C, with 5% CO_2 in the air. Human recombinant TGF-β1 was purchased from Abcam (Cambridge, UK). The choice of the concentration of TGF-β1 used in this study, that is, 10 µM, was based on previous reports.[74,75]

2.3 | RNA isolation and quantitative polymerase chain reaction (qPCR)

Total RNA was extracted from cells and converted directly into cDNA using an EZ-press Cell to cDNA Kit (B0003C, EZ Bioscience, Roseville, CA, USA). The mRNA abundance was evaluated by SYBR Green qPCR Master Mix (A0001-R, EZ Bioscience). The expression of target genes was measured by quantifying the mRNA abundance, and the expression values were normalized to the expression of GAPDH. The names of genes and their primers are listed in Table S2.

2.4 | Western blot analysis

For total protein extraction, we added 60–100 µL of Radio-Immunoprecipitation Assay (RIPA) buffer (Yeasen Biotech, Shanghai, China) containing 1% protease inhibitor (Yeasen) onto cells seeded in 6-well plates and incubated on ice for 30 minutes. The cells were scraped, and the cell-RIPA mixture was centrifuged at ~13 400 g for 10 min at 4°C to rid of cell debris. Protein concentration was determined using bicinchoninic acid (BCA) protein quantitative analysis kit (Beyotime Biotech, Shanghai, China). Protein samples were loaded on a 10% SDS-PAGE and transferred to 0.22 µm polyvinyl difluoride (PVDF) membranes (EMD Millipore, Merck, Darmstadt, Germany). The membranes were then incubated with the primary antibodies at 4°C overnight. The information on primary antibodies is listed in Table S3. After the membranes were incubated with secondary antibodies on a shaker for 1.5 h at room temperature, the signals were detected with enhanced chemiluminescence (ECL) kit (New Cell & Molecular Biotech, Suzhou, China) and digitized on Image Quant LAS 4000 mini (GE, Boston, MA, USA). Image quantification was performed using Image J software (Version 1.53a, downloaded from https://imagej.net/Downloads).

2.5 | Animals

Twenty-four 6-week-old virgin female Balb/C mice were purchased from the Shanghai Jiesijie Experimental Animal Company. All mice were maintained under a controlled environment with 22–25°C, a 12/12-h light/dark cycle, and free access to feed and water. All experiments were performed under the US National Research Council's Guide for the Care and Use of Laboratory Animals[76] and were approved by the Institutional Experimental Animals Review Committee of our hospital.

2.6 | Experimental protocol: HDAC8 selective inhibitor

A total of 24 6-week-old virgin female Balb/C mice were used. Among the 24 female adult Balb/C mice, eight were randomly selected as donors. The remaining 16 were recipients that received intraperitoneal (i.p.) injection of uterine fragments and infusion of substance P to establish a mouse model of deep endometriosis.[77] Sensory nerve-derived neuropeptides such as substance P have been shown to promote lesional progression and fibrogenesis through EMT, FMT, and SMM,[78,79] and the DE mouse model demonstrates extensive fibrosis and other features that are consistent with the human DE.[15] We designated Day 0 as the induction day when mice received an (i.p.) injection of uterine fragments. On Day −1, mice were inserted with Alzet osmotic pumps (Model 1004. DURECT Corp, Cupertino, CA, USA) containing substance P (0.1 mg/kg/day, ab120170, Abcam). The pump ensured the uniform and controlled release of contents within. As reported

TABLE 1 Characteristics of recruited patients in different groups.

Variable	Controls (n=24)	Ovarian endometrioma (n=38)	Deep endometriosis (n=20)
Age (in years)	Mean=35.9 (SD=5.5) median=35; range=28–44	Mean=34.6[NS] (SD=6.5) median=33; range=24–49	Mean=38.4[NS] (SD=7.0) median=36.5; range=29–49
Menstrual phase			
Proliferative	14 (58.3%)	18 (47.4%)[NS]	10 (50.0%)[NS]
Secretory	10 (41.7%)	20 (52.6%)	10 (50.0%)
Parity			
0	11 (45.8%)	18 (47.3%)[NS]	7 (35.0%)[NS]
1	8 (33.3%)	17 (44.7%)	12 (60.0%)
≥2	5 (20.8%)	3 (7.9%)	1 (5.0%)
Severity of dysmenorrhea			
None	24 (100.0%)	18 (47.4%)***	5 (25.0%)***
Mild	0 (0.0%)	10 (26.3%)	6 (30.0%)
Moderate	0 (0.0%)	7 (18.4%)	9 (45.0%)
Severe	0 (0.0%)	3 (7.9%)	0 (0.0%)
rASRM Stage			
I	NA	1 (2.7%)	0 (0.0%)
II		10 (27.0%)	0 (0.0%)
III		15 (40.5%)	0 (0.0%)
IV		11 (29.7%) (1 missing)	20 (100.0%)
Lesion size (mm)	NA	Mean=70.1 (SD=18.3); median=69; range=35–123 (4 missing)	Mean=14.4 (SD=14.1); median=10; range=3–50 (6 missing)
Co-occurrence of OE			
No	24 (100.0%)	NA	20 (100.0%)
Yes	0 (0.0%)		0 (0.0%)
Co-occurrence of DE			
No	24 (100.0%)	36 (94.7%)	NA
Yes	0 (0.0%)	2 (5.3%)	
Co-occurrence of adenomyosis			
No	24 (100.0%)	38 (100.0%)	18 (90.0%)
Yes	0 (0.0%)	6 (0.0%)	2 (10.0%)
Co-occurrence of fibroids			
No	24 (100.0%)	32 (84.2%)[NS]	10 (50.0%)***
Yes	0 (0.0%)	6 (15.8%)	10 (50.0%)

Note: The comparison was made in reference to the control group. Symbols for statistical significance levels: NS: $p > 0.05$; ***: $p < 0.001$. Location of DE lesions: 6 (30%) in uterosacral ligament, 4 (20%) in rectovaginal septum, 3 (15%) in peritoneal reflection, 2 (10%) in pelvic wall, 1 (5%) each in rectum, the infundibulopelvic ligament, and the posterior wall of uterus, and 2 (10%) had missing information.

Abbreviations: DE, deep endometriosis; OE, ovarian endometriomas; SD, standard deviation.

previously,[80] after anesthesia via i.p. injection of 2% chloral hydrate (v/w), we inserted the osmotic pumps on the nape of the recipient mice.

The recipient mice were randomly divided into two equal-sized groups, the control and PCI-34051. PCI-34051 (HDAC8 $IC_{50} = 10$ nM), which has >200-fold selectivity over the other HDAC

isoforms,[81] is by far the most widely used selective inhibitor of HDAC8.[82] On Day 0, all donor mice were sacrificed, and their uteri were harvested. To induce endometriosis, uterine tissues harvested from one donor mouse were processed and then injected i.p. into two recipient mice, one from each group. PCI-34051 was dissolved in normal saline containing 5% DMSO (Sigma-Aldrich), 30% PEG300 (Sangon Biotech, Shanghai, China), and 0.5% Tween80 (Saiguo Biotech, Guangzhou, China). Four weeks after the induction of deep endometriosis, mice in the PCI-34051 group were i.p. administrated with PCI-34051 (20 mg/kg/day, S2012, Selleck, Houston, TX, USA), while mice in the control group received equal volume of vehicle for 2 weeks.

All mice were sacrificed by cervical dislocation 6 weeks after the induction of deep endometriosis. The abdominal cavities were immediately cut open, and all visible lesions were carefully excised. The total weight of lesions from each mouse was weighed and fixed immediately in fixative and embedded in paraffin for histological and immunohistochemical analyses. Bodyweight and hotplate latency were evaluated before induction, intervention, and sacrifice.

2.7 | Induction of endometriosis

A well-established mouse model of endometriosis by i.p. injection of uterine fragments was used as reported previously.[80] Briefly, after 1 week of acclimatization, the donor mice received an intramuscular (i.m.) injection of estradiol benzoate (3 μg/mouse; Animal Medicine Factory, Hangzhou, China) twice a week to stimulate endometrial growth. One week later, these donor mice were sacrificed by cervical dislocation, and their uteri were harvested. The harvested uterine tissues were seeded in a Petri dish (Corning, Corning, NY, USA) containing warm sterile normal saline, split longitudinally with a pair of scissors, and minced until each fragment was no larger than 1 mm^3. The fragments were then i.p. injected into the abdominal of the recipient mice. To minimize any potential bias, the uterine fragments from one donor mouse were divided into two equal parts, with each i.p. injected into one mouse from each experimental group.

2.8 | Hotplate test

To evaluate the evoked pain behavior resulting from induced endometriosis, the hotplate test was administrated to all mice using a commercial Hotplate Analgesia Meter (Model BME-480, Institute of Biomedical Engineering, Chinese Academy of Medical Sciences, Tianjin, China) as reported previously.[23] Briefly, all mice were allowed to acclimatize for 10 min before the test. The withdrawal latencies to thermal stimulation were determined according to the following criteria: shaking or licking its hind paws or jumping on the hotplate from the moment we initially placed the mouse into the cylinder. The latency was measured twice and then averaged by a 1-h interval.

2.9 | Immunohistochemistry (IHC)

All tissue samples were fixed with 10% formalin fixative and paraffin-embedded. Serial 4 μm sections were obtained from tissue samples. We applied the first slide for H&E staining for pathological confirmation and the subsequent slides for Masson trichrome staining and IHC analysis. The vendor's names and catalog numbers of these antibodies and the dilution ratios are listed in Table S4.

Routine deparaffinization and rehydration procedures were performed. For antigen retrieval, all the slides were heated at high temperature and high pressure in citrate buffer (pH 6.0) or EDTA (pH 8.0) (Servicebio, Wuhan, China) for 3 min and then cooled to room temperature naturally. The slides were then incubated with the primary antibodies overnight at 4°C. The next day, the slides were allowed to rewarm for 1 h at room temperature before incubating them with HRP-labeled goat antirabbit/mouse IgG antibodies (JieHao Biotech, Shanghai, China) at room temperature for 1 h. After the slides were rinsed, they were stained with Diaminobenzidine (DAB) Detection Reagent (JieHao) for 1–3 min until appropriate for microscopic examination and then counterstained with hematoxylin (30 s) and mounted. Images were obtained with the microscope (Olympus BX53; Olympus, Tokyo, Japan) fitted with a digital camera (Olympus DP73; Olympus). Three to five randomly selected images at a certain magnification of each sample slide were taken to obtain a mean optional density value by Image Pro-Plus 6.0 (Media Cybernetics, Inc., Bethesda, MA, USA) as described previously.[15]

For positive control, different tissue slides were used for different antibodies according to the vendor's informative sheet. For negative controls, tissue samples were incubated with rabbit or mouse serum instead of primary antibodies. The representative photomicrographs for positive and negative control are provided in Figure S1.

2.10 | Masson trichrome staining

Masson trichrome staining was performed to quantify the proportion of collagen fibers within the tissue samples of interest as reported previously.[15] Tissue sections were deparaffinized, rehydrated, and immersed in Bouin's solution (75 mL of saturated picric acid, 25 mL of 10% formalin solution, and 5 mL of acetic acid) at 37°C for 2 h. Under the manufacturer's instructions, sections were then stained using Masson's Trichrome Staining kit (Servicebio). The area of regions where the collagen fiber layer stained blue in proportion to the entire field area within the tissue was measured using Image Pro-Plus 6.0.

2.11 | Statistical analysis

The comparison of distributions of continuous variables among over 2 groups was made using the Kruskal test. The paired Wilcoxon's rank-sum test ($n \geq 5$) and paired t-test ($n < 5$) were employed to compare two paired groups. Wilcoxon's rank test ($n \geq 5$) and t-test ($n < 5$)

were employed to compare two independent groups. Pearson's or Spearman's rank correlation coefficient was used when evaluating correlations between two variables when both variables were continuous or when at least one variable was ordinal. To evaluate which factors were associated with the staining levels, multiple linear regression analysis was used, incorporating age, menstrual phase, co-occurrence of adenomyosis or of uterine fibroids, and whether the patient had OE or DE as covariables. p-Values of <0.05 were considered statistically significant. All computations were made with R version 4.2.2.[83]

3 | RESULTS

3.1 | Changes in expression pattern of HDACs in endometriotic cells resulting from TGF-β1 stimulation

TGF-β1 is the archetypical profibrotic cytokine and a driver of EMT, FMT, and SMM in endometriosis.[70] As an initial screening, we first evaluated the expression patterns of the Zn^{2+}-dependent HDAC family (HDAC1-11) in endometriotic cells after TGF-β1-induced EMT, FMT, and SMM. As shown previously, TGF-β1 treatment induced EMT, FMT, and SMM in endometriotic cells[70,71] (Figure S2). We first treated the endometriotic epithelial cell line 11Z with TGF-β1 for 72h to induce EMT. We found that TGF-β1 induced a significant increase in gene expression of HDAC1, HDAC2, HDAC3, HDAC8, and HDAC6 while other members of HDACs were not affected (Figure 1A). Consistently, similar changes in protein levels of HDAC1, HDAC2, HDAC3, HDAC8, and HDAC6 were also observed (Figure 1B).

We next treated primary human endometriotic stromal cells (hESCs) derived from OE lesions with TGF-β1 for 3 and 15days, respectively, to induce FMT and SMM, as shown previously.[70] We found that the treatment significantly increased gene expression levels of HDAC2, HDAC3, and HDAC6 in hESCs during FMT and SMM processes (Figure 1C,D), which were confirmed by Western blot analysis (Figure 1E). These results suggest that TGF-β1 regulates select members of the Zn^{2+}-dependent HDAC family in endometriotic cells, and this regulation appears to be cell-type-dependent. Thus, we decided to further evaluate all members of Class I and one member of Class II HDACs, that is, HDAC6, and their possible roles in the progression and fibrogenesis in endometriosis.

3.2 | Differential expression of class I HDACs and HDAC6 in OE and DE lesions

Next, we assessed the immunoreactivity of Class I HDACs, and HDAC6 in endometriotic tissues from patients with OE and DE, as well as normal endometrium from controls. The characteristics of the recruited patients with OE and DE, and the control paricipants are listed in Table 1.

We evaluated the lesional staining levels separately for glandular epithelial and stromal components. The cell types of positive-staining cells and the localization of stained cells are listed in Table 2.

The HDAC1 and HDAC2 staining was both localized in the nucleus, while that of HDAC3 and HDAC8 was localized in the nucleus and cytoplasm, and that of HDAC6 was localized in the cytoplasm of the epithelial and stromal cells (Figure 2). To control for possible confounding and to account for comorbidity, we employed multiple linear regression analyses when analyzing the lesional staining levels and the extent of lesional fibrosis using age, parity, menstrual phase, co-occurrence of OE, DE, adenomyosis, and uterine fibroids as covariables.

We found that overall there are different staining levels between different cellular components as well as between OE and DE tissues. However, lesional staining of HDAC2 was consistently reduced in both epithelial and stromal components (all p-values ≤ 0.023; Table 2 and Figure 2). In contrast, lesional staining of HDAC8 was consistently elevated in both epithelial and stromal components (all p-values ≤ 0.0032; Table 2 and Figure 2). In addition, while in DE lesions the staining levels of HDAC1 and HDAC6 in both epithelial and stromal components were significantly elevated (all p-values ≤ 0.028) but that of HDAC3 were significantly reduced (all p-values ≤ 0.013), their staining levels in OE samples were either similar to control endometrium or different from those of DE samples (Table 2 and Figure 2). This discrepancy may be attributable to the difference in the extent of lesional fibrosis and thus the tissue rigidity or difference in functions in different cellular components. Regardless, our data consistently demonstrate the HDAC8 appears to be elevated in the entire progression course.

Consistent with our previous results,[15] we found that both OE and DE lesions exhibit a significant increase in the fibrotic content compared to control endometrium (both p-values ≤ 4.0 × 10^{-15}; Table 2 and Figure 2), and the extent of fibrosis was even higher in DE as compared with OE.

Next, we analyzed the correlation between the extent of lesional fibrosis and lesional staining of various HDACs. We found that the extent of lesional fibrosis correlated positively with the lesional staining of HDAC1 in the epithelial component ($r=0.60$, $p=8.8 \times 10^{-9}$; Figure 3A) but negatively with that of HDAC2 in both epithelial and stromal components ($r=-0.61$, $p=5.6 \times 10^{-9}$; Figure 3B; $r=-0.61$, $p=0.3 \times 10^{-9}$; Figure 3C, respectively) and with that of HDAC3 in the epithelial component ($r=-0.28$, 0.014; Figure 3D). In addition, the extent of lesional fibrosis correlated positively with the lesional staining of HDAC8 and HDAC6 in both the epithelial and stromal components ($r=0.64$, $p=2.7 \times 10^{-10}$, $r=0.75$, $p=2.3 \times 10^{-15}$, $r=0.59$, $p=2.0 \times 10^{-8}$, $r=0.41$, $p=2.3 \times 10^{-4}$, respectively; Figure 3E–H). Of note, these correlations were consistent with what we observed in serially harvested lesions from mice with induced endometriosis.[72]

3.3 | Confirmation by gene and protein analysis

To further confirm our IHC findings, we prepared primary endometrial stromal cells that were separated from the normal endometrium (NESCs) and endometriotic stromal cells derived from OE lesions (EESCs), and evaluated both the gene and protein expression levels of HDAC1, HDAC2, HDAC3, HDAC8, and HDAC6 in NESCs and
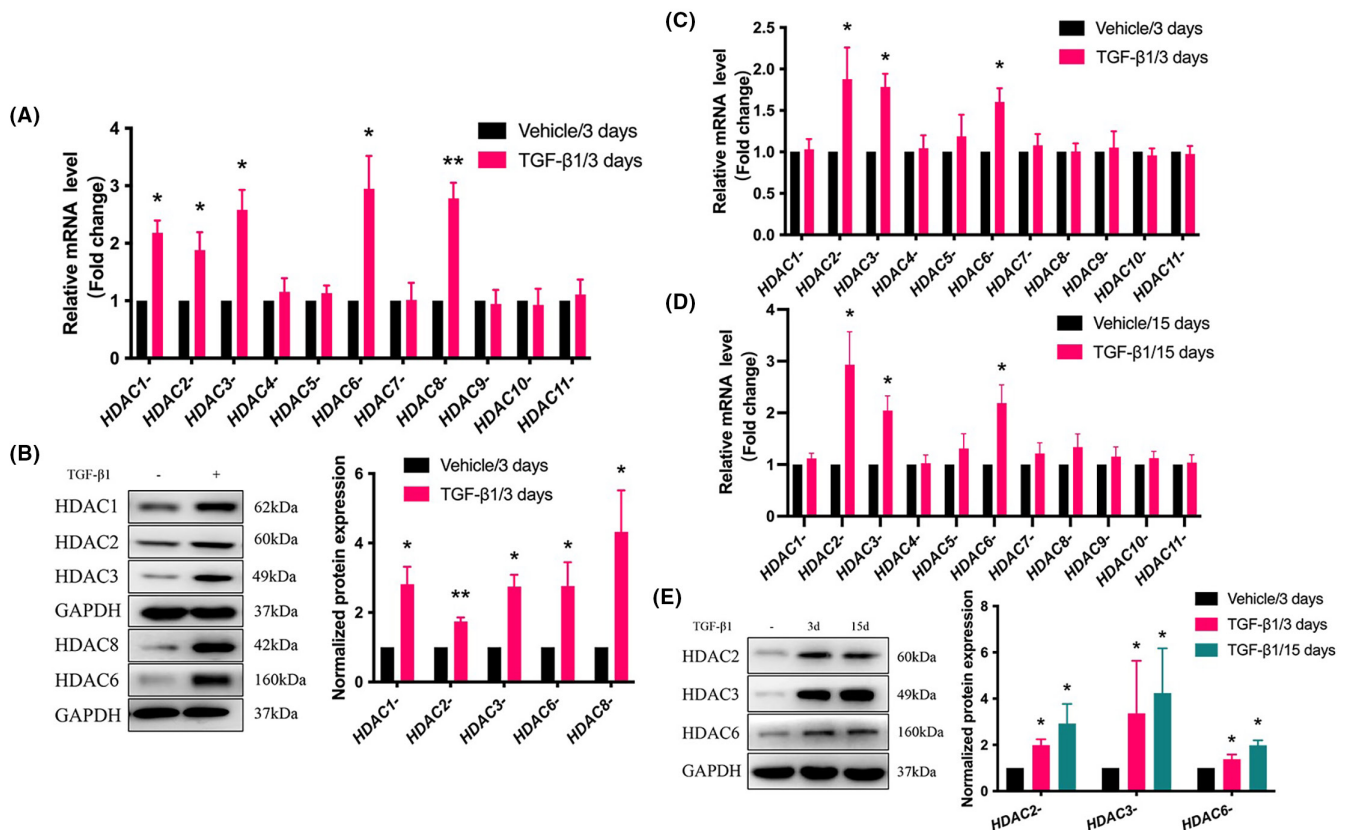
FIGURE 1 Expression of histone deacetylases (HDACs) in transforming growth factor-β1 (TGF-β1)-induced EMT, FMT, and SMM in endometriotic cells. (A) 11Z cells were cultured with vehicle (PBS) or TGF-β1 (10 ng/mL) for 72 h to induce EMT, and the mRNA expression levels of the Zn^{2+}-dependent HDAC family (11 isoforms) were detected by qPCR ($N = 3$). (B) Western blot detection (left panel) and data analysis (right panel) of HDAC1, HDAC2, HDAC3, HDAC8, and HDAC6 in 11Z cells cultured with vehicle or TGF-β1 (10 ng/mL) for 72 h ($N = 3$). (C) Primary endometriotic stromal cells (hESCs) cells were cultured with vehicle or TGF-β1 (10 ng/mL) for 3 days to induce FMT; (D) hESCs cells were cultured with vehicle or TGF-β1 (10 ng/mL) for 15 days to induce SMM, and the mRNA expression levels of the Zn^{2+}-dependent HDAC family (11 isoforms) were detected by qPCR ($N = 6$). (E) Western blot detection (left panel) and data analysis (right panel) of HDAC2, HDAC3, and HDAC6 in hESCs cells cultured with vehicle or TGF-β1 (10 ng/mL) for 3 and 15 days ($N = 6$). Gene and protein expression levels were normalized to GAPDH expression. The data are represented by the means ± SDs. Symbols of statistical significance levels: *$p < 0.05$; **$p < 0.01$. Student t-test was used in panels (A) and (B) and Wilcoxon matched-paired signed-rank test was used in panels (C), (D), and (E).

TABLE 2 List of immunohistochemistry markers, along with their distribution in different cell types, and the location in which the scoring was performed, along with the results of multiple linear regression analyses.

Marker name	Component	Location of the staining	OE	DE	R^2
HDAC1	Epithelium	N	NS	↑	0.06
	Stroma		↓	↑↑	0.27
HDAC2	Epithelium	N	↓↓↓	↓↓↓	0.65
	Stroma		↓↓↓	↓	0.58
HDAC3	Epithelium	N+C	↑↑↑	↓	0.51
	Stroma		NS	↓↓↓	0.23
HDAC8	Epithelium	N+C	↑↑	↑↑↑	0.29
	Stroma		↑↑	↑↑↑	0.60
HDAC6	Epithelium	C	NS	↑↑↑	0.48
	Stroma		NS	↑↑	0.24
Extent of fibrosis	Entire lesion		↑↑↑	↑↑↑	0.70

Note: ↓: Significant decrease; ↑: Significant increase. The number of arrows indicates the significance level, for example, ↑: $p < 0.05$; ↑↑: $p < 0.01$; ↑↑↑: $p < 0.001$.

Abbreviations: C, cytoplasm; DE, deep endometriosis; N, nuclear; OE, ovarian endometriomas.
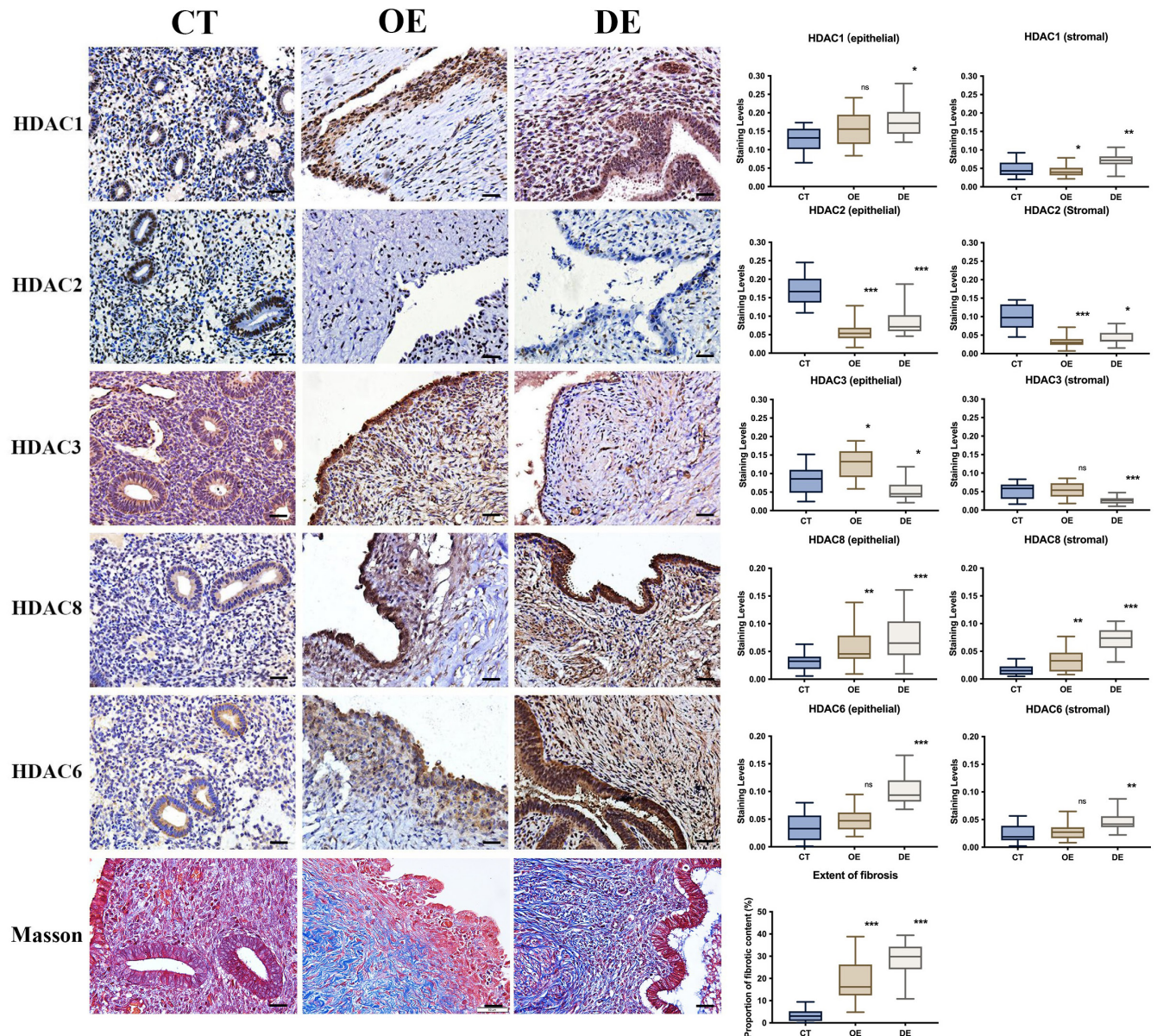
FIGURE 2 Representative photomicrographs of the immunostaining of HDAC1, HDAC2, HDAC3, HDAC8, and HDAC6, and Masson trichrome staining in control endometrium (CT), ovarian endometrioma (OE), and deep endometriosis (DE) tissue samples. Different rows show different markers as indicated. Different columns represent different tissue samples. In all figures, magnification: ×400. Scale bar = 50 μm. Box plots summarizing the difference in HDAC1, HDAC2, HDAC3, HDAC8, and HDAC6, and the extent of fibrosis in control endometrium (CT), ovarian endometrioma (OE), and deep endometriosis (DE) tissue samples. The staining level was evaluated in glandular epithelial and stromal components, respectively. The data are represented by the means ± SDs. Symbols of statistical significance levels: $*p < 0.05$; $**p < 0.01$; $***p < 0.001$; ns: not statistically significant ($p > 0.05$). Multiple linear regression analyses were used.

EESCs by qPCR and Western blot (Figure 4A). The characteristics of the recruited patients with OE and the control participants are listed in Table S1. We found that, compared with NESCs, EESCs had significantly elevated gene expression levels of HDAC1 and HDAC8 and significantly reduced expression of HDAC2 and HDAC3 (all p-values < 0.0044; Figure 4B). However, there was no significant difference in the expression level of HDAC6 ($p = 0.19$; Figure 4B). Western blot analysis confirmed significantly elevated protein expression levels of HDAC1 and HDAC8 ($p = 0.006$ and $p < 0.001$, respectively), reduced levels of HDAC2 and HDAC3 ($p = 0.0099$ and 0.048, respectively), but not HDAC6 ($p = 0.15$; Figure 4C). These

results further confirmed our IHC findings and suggested that the aberration of HDAC1-3 and HDAC8, and HDAC6 in the stroma, likely to play a vital role in endometriosis.

3.4 | Therapeutic potentials of a specific HDAC8 inhibitor

Given the results of the above ex vivo experiments and in view of the in vivo results that HDAC8 activation accelerated, while HDAC8 inhibition decelerated lesional progression and fibrogenesis,[72] we
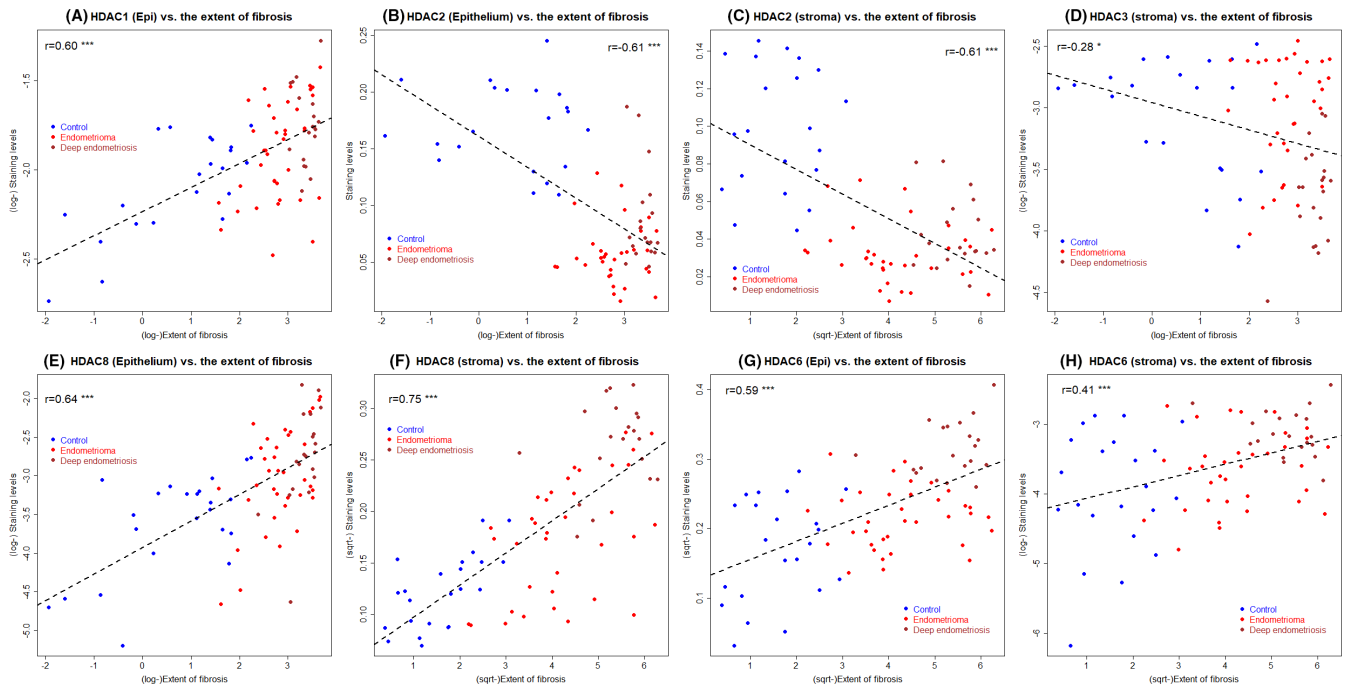
FIGURE 3 Scatter plots showing the correlation between the extent of lesional fibrosis and the staining levels of HDAC1 in the epithelial component (A), HDAC2 in the epithelial (B) and stromal components (C), HDAC3 in the stromal component (D), HDAC8 in the epithelial (E) and stromal components (F), and HDAC6 in the epithelial (G) and the stromal components (H) in control endometrium, ovarian endometrioma and deep endometriosis tissue samples. In each plot, each dot represents one data point from one patient, and the dashed line represents the regression line. Pearson's correlation coefficient, along with its *p*-value, also is shown. Symbol of statistical significance level: *$p < 0.05$; ***$p < 0.001$.
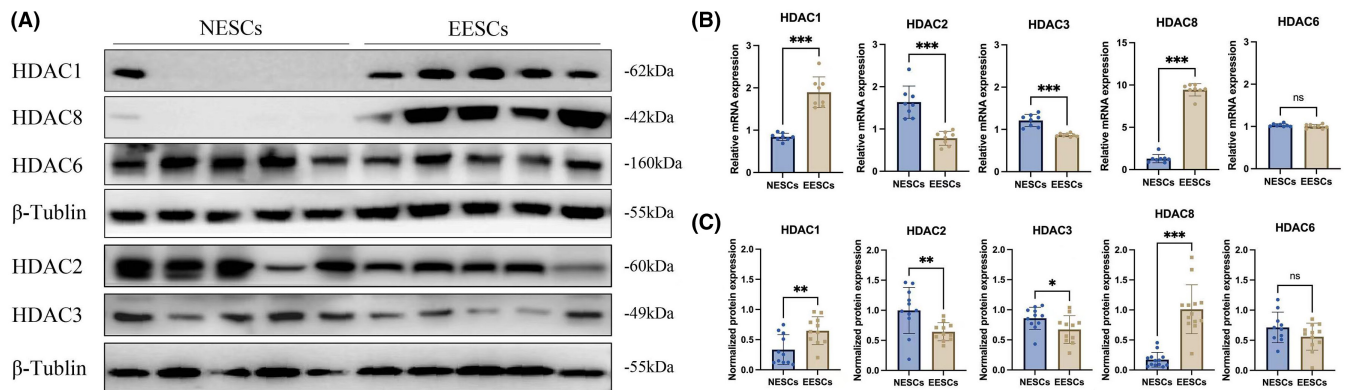
FIGURE 4 Western blot (A and C) and qPCR (B) detection of HDAC1, HDAC2, HDAC3, HDAC8, and HDAC6 expression in normal endometrium-derived stromal cells (NESCs) and ovarian endometrioma-derived stromal cells (EESCs). The data are represented by the means ± SDs. Symbols of statistical significance levels: *$p < 0.05$; **$p < 0.01$; ***$p < 0.001$; ns, not statistically significant ($p > 0.05$). $N = 11$–13 for each group. The Wilcoxon test was used.

speculated that inhibition of HDAC8 may have a therapeutic effect. Consequently, we next evaluated the potential therapeutic effect of PCI-34051 (PCI), an HDAC8-specific inhibitor, on mice with induced deep endometriosis.

No mouse died during the experiment, and no adverse effect was detected. PCI appeared to be well tolerated in treated mice. Endometriosis was successfully induced and histologically confirmed by H&E staining. There was no difference in bodyweight among all groups of mice before and after the successful induction of deep endometriosis (all *p*-values ≥ 0.56; Figure 5A).

We also evaluated the pain behavior of all mice using the hot-plate test. As expected, we found no difference in hotplate latency before the start of induction and before the start of the treatment (both *p*-values ≥ 0.43; Figure 5B), even though the latency was significantly shortened in both groups due to the presence of deep endometriosis (both *p*-values = 0.008). After 2 weeks of treatment, mice treated with PCI had significantly longer latency than that of control mice ($p = 0.005$; Figure 5B).

We found no visible endometriotic lesions in one PCI-treated mouse. The lesion weight correlated positively with the hotplate
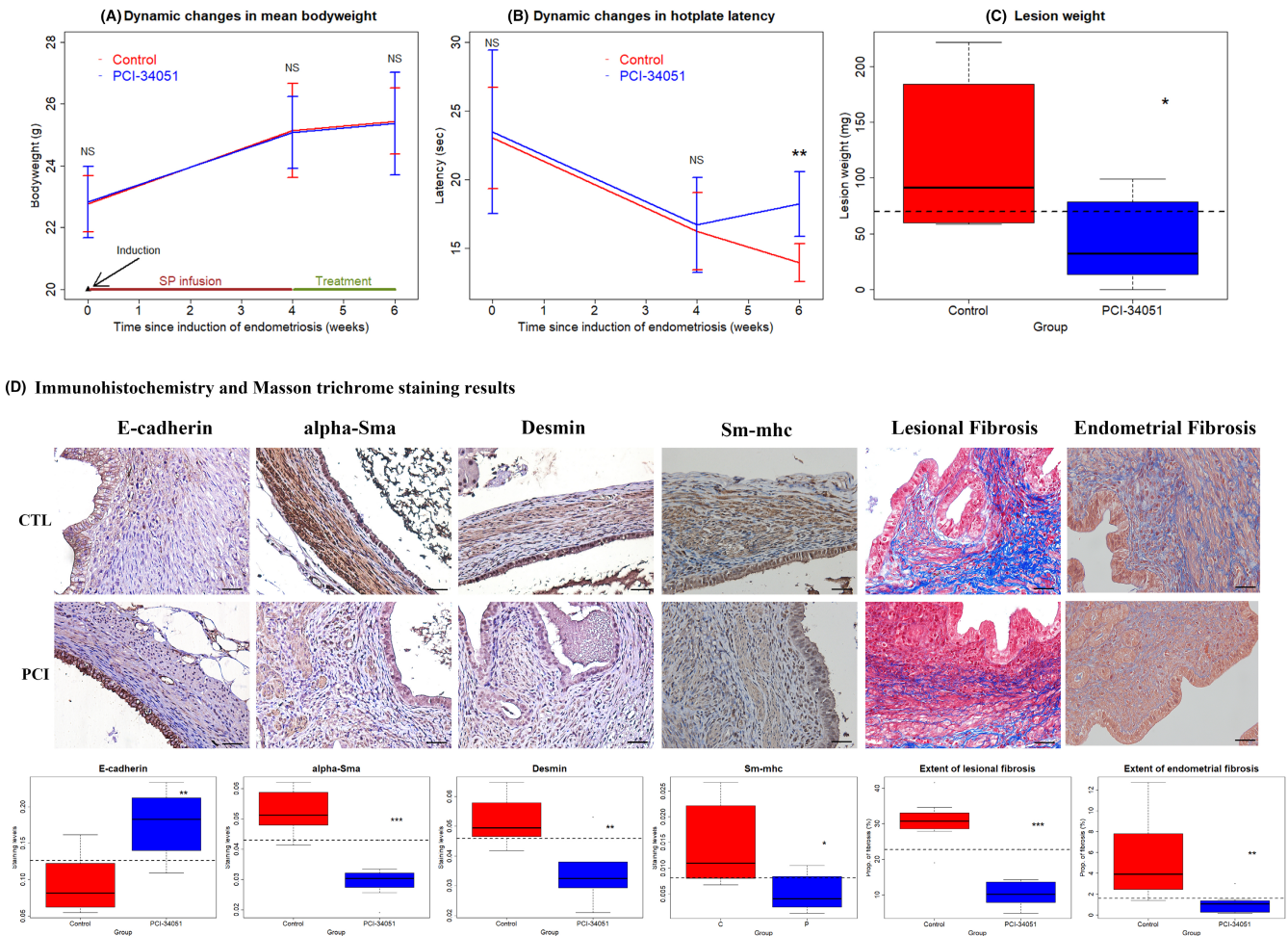
FIGURE 5 Dynamic changes in the mean bodyweight (A) and the mean hotplate plate latency (B) between two groups of mice. In both (A) and (B), the data are represented by the means ± SDs, and the time point at which deep endometriosis was induced is indicated by an arrow. The start time and the duration of the treatment of specific HDAC8 inhibitor (PCI-34051, 20 mg/kg/d) or vehicle also is indicated. (C) Boxplot showing the total lesion weight between two groups of mice. The dashed line is the median value of the two groups. (D) Representative photomicrographs of immunostaining and Masson trichrome staining analysis of endometriotic lesions and endometrial tissues from two groups. Different rows show different tissue samples from control mice (CTL) and mice treated with PCI-34051 (PCI). Different columns represent different markers as indicated. In Masson trichrome staining, the collagen fibers in lesions were stained blue. In all figures, magnification = ×400. Scale bar = 50 μm. Boxplot of staining levels of E-cadherin, α-Sma, desmin, Sm-mhc and the extent of lesional and endometrial fibrosis in lesions or endometrial tissues from control mice and mice treated with PCI-34051, respectively. The dashed line is the median value of all groups. Symbols of statistical significance levels: *$p < 0.05$; **$p < 0.01$; ***$p < 0.001$; NS, not statistically significant ($p > 0.05$).

latency ($r = -0.74$, $p = 0.001$). Compared with the control mice, the average lesion weight in PCI group was reduced by 63.6% (43.3 ± 36.9 vs. 118.8 ± 69.2 mg; Figure 5C).

To gain insight into the possible mechanisms underlying the suppressive effect of the above inhibitors, we also performed IHC analyses. We analyzed the expression of E-cadherin (a marker for epithelial cells), α-Sma (a marker for myofibroblasts), desmin, and smooth muscle myosin heavy chain (Sm-mhc (two markers of highly differentiated smooth muscle cells or SMCs) in ectopic lesions. In addition, we evaluated the extent of lesional as well as endometrial fibrosis by Masson trichrome staining. E-cadherin staining was seen mostly in the cytoplasm and membranes in epithelial cells, and that of α-Sma, desmin, and Sm-mhc was in the cytoplasm in both stromal and epithelial cells (Figure 5D).

We found that treatment with PCI significantly increased the lesional staining of E-cadherin ($p = 0.006$) but significantly reduced the lesional staining of α-Sma ($p = 0.0006$), desmin ($p = 0.006$), Sm-mhc ($p = 0.021$), as well as the extent of lesional and endometrial fibrosis ($p = 0.0006$ and $p = 0.0011$, respectively; Figure 5D).

The extent of lesional fibrosis correlated positively with that of endometrium ($r = 0.56$, $p = 0.029$). As expected, the extent of lesional fibrosis correlated negatively with the E-cadherin staining ($r = -0.54$, $p = 0.036$) but positively with the staining levels of α-Sma ($r = 0.89$, $p = 9.1 \times 10^{-6}$), and desmin ($r = 0.54$, $p = 0.038$). It also correlated positively with the lesion weight ($r = 0.81$, $p = 0.0002$) but negatively with the hotplate latency ($r = -0.87$, $p = 2.7 \times 10^{-5}$).

4 | DISCUSSION

In this study, we found a significant elevation in HDAC8 immunostaining in both OE and DE lesions as compared with normal endometrium. Consistently, we also found significantly increased gene and protein expression levels of HDAC8 in endometriotic stromal cells derived from OE lesions. For other Class I HDACs and HDAC6, their lesional expression was more subtle and nuanced. HDAC1 and HDAC6 staining was significantly elevated in DE lesions while HDAC2 and HDAC3 staining in DE lesions was significantly reduced. Consistently, the gene and protein expression levels of both HDAC2 and HDAC3 were significantly reduced while that of HDAC1, but not HDAC6, were significantly elevated in endometriotic stromal cells derived from OE lesions (Table 2 and Figure 4). In addition, we found that treatment of mice with induced deep endometriosis with an HDAC8 inhibitor resulted in significantly longer hotplate latency, a reduction of lesion weight by nearly two-thirds, and significantly reduced lesional fibrosis, all suggestive of remarkable therapeutic potential.

While aberrant expression of HDAC8 has so far not been reported in endometriosis to our best knowledge, our finding that HDAC1 expression is elevated in OE and, in particular, DE lesions is consistent with the previous reports.[8,52] However, our finding that HDAC2 is downregulated in endometriotic lesions is at direct odds with either Colón-Díaz et al. who reported lesional overexpression of HDAC2[52] or Samartzis et al., who found no change.[8] It also is in conflict with the result of our own screening results (Figure 1).

However, our results of reduced HDAC2 and HDAC3 expression in endometriotic lesions, especially in DE lesions, are consistent with the report that increased substrate stiffness reduces the HDAC2 expression.[84] Indeed, as endometriotic lesions progress, they exhibit increased fibrotic content and thus increased tissue stiffness, rendering easier detection by elastography.[85] In particular, DE lesions are known to be more fibrotic and thus stiffer than OE lesions.[15] Since cells can transduce chemical as well as mechanical cues from their local microenvironment and further relay these signals into the nucleus to change the epigenetic state and regulate gene expression, nucleus can effectively act as a mechanosensor by undergoing deformation in the presence of mechanical forces, leading to altered chromatin organization, epigenetic modifications, gene expression, and, finally, phenotypic changes.[86,87] Consequently, there is reason to believe that both HDAC2 and HDAC3 expression is reduced as endometriotic lesions become more fibrotic, especially in DE lesions as reported here, in particular given the report that both HDAC2 and HDAC3 are constitutively expressed in normal endometrium.[88] This may also be supported by the report that HDAC3 overexpression in conjunction with estrogen-ERα suppresses STING endometrial epithelial cells[89] yet STING is upregulated in ectopic endometrium.[90]

Indeed, we found that culturing an endometrial epithelial cell line in high-stiff substrates resulted in downregulation of HDAC3,[91] which may account for reduced endometrial HDAC3 expression

in infertile women with endometriosis.[92] Viewed from this vista, the discrepancy between the screening results (Figure 1) and IHC (Figure 2) and in vitro results (Figure 4) could be attributable to the failure to recapitulate faithfully the in vivo lesional microenvironment in the screening experiment. This, along with the recent findings of diminished PGE2 signaling as lesions become more fibrotic,[93,94] underscores the fact that not all endometriotic lesions are equal[36] and that many molecular aberrations in endometriosis are quite subtle and nuanced, depending critically on the developmental stages of lesions. In addition, the discrepancy between our screening and later IHC results underscores the importance of the faithful recapitulation of the in vivo lesional environment: it is important to consider not only the stimulant but also the rigidity of the culture substrate.

Our finding of lesional HDAC8 overexpression appears to be in agreement with the report that HDAC8 is exclusively expressed by cells showing smooth muscle cell (SMC) differentiation[95] and is essential for SMC contractility.[96] This is consistent with the suppression of both lesional and endometrial fibrosis in mice treated with the HDAC8 inhibitor as well as our mouse data that demonstrated increasing HDAC8 staining in later stage of endometriosis,[72] since both FMT and SMM are two integral parts in lesional progression and fibrogenesis.[45,70,71] Consistently, the treatment of mice with induced deep endometriosis with an HDAC8 inhibitor exhibited remarkable therapeutic potential.

Similar to HDAC8, aberrant expression of HDAC6 in endometriosis has not been reported so far. However, somatic inactivating mutation at ARID1A in endometriosis has been reported.[97–99] ARID1A mutation in endometriotic epithelial cells has been found to be associated with the upregulation of pro-angiogenic and pro-lymphangiogenic factors and remodeling of the endothelial cell compartment, with enrichment of lymphatic endothelial cells.[100] Interestingly, at least in ovarian cancer, ARID1A mutation inactivates the apoptosis-promoting function of p53 by upregulating HDAC6,[101] and HDAC6 increases M2 polarization of macrophages through GATA3/IL-10.[102]

Regardless, the roles of both HDAC6 and HDAC8 in various fibrotic diseases have been well-documented.[103,104] In contrast to the therapeutic effect resulting from the inhibition of HDAC8 as demonstrated by this study, the administration of an HDAC8 activator accelerated lesional progression and fibrogenesis through promoting FMT and proliferation.[72] The work is ongoing to further elucidate the mechanisms underlying HDAC8-facilitated lesional progression.

VPA is known to inhibit Class I (HDAC1-3 and 8) and Class IIa (HDAC4-5, 7, and 9) HDACs.[50,51] Since HDAC8 belongs to the Class I HDAC family, the encouraging therapeutic potential of inhibiting HDAC8 as demonstrated in this study provides another reason as why VPA has been shown to be of therapeutic potential in endometriosis[18,21] as well as in adenomyosis.[22,24,32]

Our study has several strengths. First, we used a combination of in vitro screening, IHC, and in vitro gene and protein expression analyses, as well as in vivo experimentation to confirm as well as to discern different results, highlighting the subtlties and nuances

in lesional aberration of Class I HDACs and HDAC6. Second, we evaluated the IHC staining separately for OE and DE lesions, the two subtypes of endometriosis that are known to have substantial histological differences[15] and pathophysiology.[78,79] Lastly, capitalizing on the upregulation of HDAC8 in lesions as demonstrated by both in vitro and in vivo experiments and its possible role in FMT, we demonstrated the therapeutic potential of HDAC8 suppression in a mouse model of deep endometriosis, a subtype of endometriosis that is known to be quite challenging to manage by medication.[105]

Our study also has several limitations. First, it is confined by the use of histologic and immunohistochemistry analyses and limited molecular data, as well as the lack of mechanistic data. Second, despite positive results from IHC and our mouse experiment, we did not further investigate whether the negative finding of HDAC6 from the gene and protein expression study is due to the use of culture substrate, nor did we provide further evidence to show that the discrepancy between the screening and the IHC analysis is truly the failure in recapitulating the in vivo lesional microenvironment. Lastly, we did not measurement of HDAC activities. Further investigations are warranted to illuminate these issues.

In summary, we demonstrated the overexpression of HDAC8 in endometriotic lesions and found nuanced aberrations in HDAC1, HDAC2, HDAC3, and HDAC6. On these findings, we demonstrated that treatment of an HDAC8 inhibitor in mice with induced deep endometriosis exhibited promising therapeutic efficacy. Our results rectify the previous report of higher or no change in HDAC2 expression in endometriosis, and we also report that all Class I HDACs, plus HDAC6, are aberrantly expressed in endometriosis. These findings highlight the progression-dependent nature of these aberrations, and demonstrate, for the first time, the therapeutic potential of suppressing HDAC8, calling for more research on HDACs in endometriosis.

CONFLICT OF INTEREST STATEMENT

S.W.G. is a member of the Scientific Advisory Board of Heranova BioSciences and has provided consultancy advice to the company, as well as to Sound Bioventures and BioGeneration, but these activities had no bearing on this work. All authors state that they have no competing interest.

ORCID

Sun-Wei Guo https://orcid.org/0000-0002-8511-7624

REFERENCES

1. Wu Y, Halverson G, Basir Z, Strawn E, Yan P, Guo SW. Aberrant methylation at HOXA10 may be responsible for its aberrant expression in the endometrium of patients with endometriosis. Am J Obstet Gynecol. 2005;193(2):371–80.
2. Wu Y, Strawn E, Basir Z, Halverson G, Guo SW. Promoter hypermethylation of progesterone receptor isoform B (PR-B) in endometriosis. Epigenetics. 2006;1(2):106–11.
3. Xue Q, Lin Z, Cheng YH, Huang CC, Marsh E, Yin P, et al. Promoter methylation regulates estrogen receptor 2 in human endometrium and endometriosis. Biol Reprod. 2007;77(4):681–7.
4. Xue Q, Lin Z, Yin P, Milad MP, Cheng YH, Confino E, et al. Transcriptional activation of steroidogenic factor-1 by hypomethylation of the 5' CpG Island in endometriosis. J Clin Endocrinol Metab. 2007;92(8):3261–7.
5. Jichan N, Xishi L, Guo SW. Promoter hypermethylation of progesterone receptor isoform B (PR-B) in adenomyosis and its rectification by a histone deacetylase inhibitor and a demethylation agent. Reprod Sci. 2010;17(11):995–1005.
6. Izawa M, Harada T, Taniguchi F, Ohama Y, Takenaka Y, Terakawa N. An epigenetic disorder may cause aberrant expression of aromatase gene in endometriotic stromal cells. Fertil Steril. 2008;89(5 Suppl):1390–6.
7. Izawa M, Taniguchi F, Uegaki T, Takai E, Iwabe T, Terakawa N, et al. Demethylation of a nonpromoter cytosine-phosphate-guanine Island in the aromatase gene may cause the aberrant up-regulation in endometriotic tissues. Fertil Steril. 2011;95(1):33–9.
8. Samartzis EP, Noske A, Samartzis N, Fink D, Imesch P. The expression of histone deacetylase 1, but not other class I histone deacetylases, is significantly increased in endometriosis. Reprod Sci. 2013;20(12):1416–22.
9. Liu X, Nie J, Guo SW. Elevated immunoreactivity against class I histone deacetylases in adenomyosis. Gynecol Obstet Invest. 2012;74(1):50–5.
10. Wu Y, Strawn E, Basir Z, Halverson G, Guo SW. Aberrant expression of deoxyribonucleic acid methyltransferases DNMT1, DNMT3A, and DNMT3B in women with endometriosis. Fertil Steril. 2007;87(1):24–32.
11. Liu X, Guo SW. Aberrant immunoreactivity of deoxyribonucleic acid methyltransferases in adenomyosis. Gynecol Obstet Invest. 2012;74(2):100–8.

12. Ding D, Liu X, Guo SW. Overexpression of lysine-specific demethylase 1 in ovarian endometriomas and its inhibition reduces cellular proliferation, cell cycle progression, and invasiveness. Fertil Steril. 2014;101(3):740–9.

13. Sun Q, Ding D, Liu X, Guo SW. Tranylcypromine, a lysine-specific demethylase 1 (LSD1) inhibitor, suppresses lesion growth and improves generalized hyperalgesia in mouse with induced endometriosis. Reprod Biol Endocrinol. 2016;14:17.

14. Zhang Q, Dong P, Liu X, Sakuragi N, Guo SW. Enhancer of Zeste homolog 2 (EZH2) induces epithelial-mesenchymal transition in endometriosis. Sci Rep. 2017;7(1):6804.

15. Liu X, Zhang Q, Guo SW. Histological and Immunohistochemical characterization of the similarity and difference between ovarian Endometriomas and deep infiltrating endometriosis. Reprod Sci. 2018;25(3):329–40.

16. Colon-Caraballo M, Torres-Reveron A, Soto-Vargas JL, Young SL, Lessey B, Mendoza A, et al. Effects of histone methyltransferase inhibition in endometriosis. Biol Reprod. 2018;99(2):293–307.

17. Brunty S, Ray Wright K, Mitchell B, Santanam N. Peritoneal modulators of EZH2-miR-155 cross-talk in endometriosis. Int J Mol Sci. 2021;22(7):3492.

18. Wu Y, Guo SW. Histone deacetylase inhibitors trichostatin a and valproic acid induce cell cycle arrest and p21 expression in immortalized human endometrial stromal cells. Eur J Obstet Gynecol Reprod Biol. 2008;137(2):198–203.

19. Wu Y, Guo SW. Suppression of IL-1beta-induced COX-2 expression by trichostatin a (TSA) in human endometrial stromal cells. Eur J Obstet Gynecol Reprod Biol. 2007;135(1):88–93.

20. Wu Y, Starzinski-Powitz A, Guo SW. Trichostatin a, a histone deacetylase inhibitor, attenuates invasiveness and reactivates E-cadherin expression in immortalized endometriotic cells. Reprod Sci. 2007;14(4):374–82.

21. Liu M, Liu X, Zhang Y, Guo SW. Valproic acid and progestin inhibit lesion growth and reduce hyperalgesia in experimentally induced endometriosis in rats. Reprod Sci. 2012;19(4):360–73.

22. Liu X, Guo SW. Valproic acid alleviates generalized hyperalgesia in mice with induced adenomyosis. J Obstet Gynaecol Res. 2011;37(7):696–708.

23. Lu Y, Nie J, Liu X, Zheng Y, Guo SW. Trichostatin a, a histone deacetylase inhibitor, reduces lesion growth and hyperalgesia in experimentally induced endometriosis in mice. Hum Reprod. 2010;25(4):1014–25.

24. Mao X, Wang Y, Carter AV, Zhen X, Guo SW. The retardation of myometrial infiltration, reduction of uterine contractility, and alleviation of generalized hyperalgesia in mice with induced adenomyosis by levo-tetrahydropalmatine (l-THP) and andrographolide. Reprod Sci. 2011;18(10):1025–37.

25. Imesch P, Samartzis EP, Dedes KJ, Fink D, Fedier A. Histone deacetylase inhibitors down-regulate G-protein-coupled estrogen receptor and the GPER-antagonist G-15 inhibits proliferation in endometriotic cells. Fertil Steril. 2013;100(3):770–6.

26. Imesch P, Fink D, Fedier A. Romidepsin reduces histone deacetylase activity, induces acetylation of histones, inhibits proliferation, and activates apoptosis in immortalized epithelial endometriotic cells. Fertil Steril. 2010;94(7):2838–42.

27. Imesch P, Samartzis EP, Schneider M, Fink D, Fedier A. Inhibition of transcription, expression, and secretion of the vascular epithelial growth factor in human epithelial endometriotic cells by romidepsin. Fertil Steril. 2011;95(5):1579–83.

28. Seo SK, Lee JH, Chon SJ, Yun BH, Cho S, Choi YS, et al. Trichostatin a induces NAG-1 expression and apoptosis in human Endometriotic stromal cells. Reprod Sci. 2018;25(9):1349–56.

29. Kai K, Nasu K, Kawano Y, Aoyagi Y, Tsukamoto Y, Hijiya N, et al. Death receptor 6 is epigenetically silenced by histone deacetylation in endometriosis and promotes the pathogenesis of endometriosis. Am J Reprod Immunol. 2013;70(6):485–96.

30. Kawano Y, Nasu K, Hijiya N, Tsukamoto Y, Amada K, Abe W, et al. CCAAT/enhancer-binding protein alpha is epigenetically silenced by histone deacetylation in endometriosis and promotes the pathogenesis of endometriosis. J Clin Endocrinol Metab. 2013;98(9):E1474–82.

31. Kawano Y, Nasu K, Li H, Tsuno A, Abe W, Takai N, et al. Application of the histone deacetylase inhibitors for the treatment of endometriosis: histone modifications as pathogenesis and novel therapeutic target. Hum Reprod. 2011;26(9):2486–98.

32. Liu X, Guo SW. A pilot study on the off-label use of valproic acid to treat adenomyosis. Fertil Steril. 2008;89(1):246–50.

33. Xishi L, Lei Y, Guo SW. Valproic acid as a therapy for adenomyosis: a comparative case series. Reprod Sci. 2010;17(10):904–12.

34. Burla L, Kalaitzopoulos DR, Metzler JM, Scheiner D, Imesch P. Popularity of endocrine endometriosis drugs and limited alternatives in the present and foreseeable future: a survey among 1420 affected women. Eur J Obstet Gynecol Reprod Biol. 2021;262:232–8.

35. Guo SW, Groothuis PG. Is it time for a paradigm shift in drug research and development in endometriosis/adenomyosis? Hum Reprod Update. 2018;24(5):577–98.

36. Guo SW. Various types of adenomyosis and endometriosis: In search of optimal management. Fertil Steril. 2023;119:711–26.

37. Moynihan AT, Hehir MP, Sharkey AM, Robson SC, Europe-Finner GN, Morrison JJ. Histone deacetylase inhibitors and a functional potent inhibitory effect on human uterine contractility. Am J Obstet Gynecol. 2008;199(2):167. e1-7.

38. Khan S, Ahirwar K, Jena G. Anti-fibrotic effects of valproic acid: role of HDAC inhibition and associated mechanisms. Epigenomics. 2016;8(8):1087–1101.

39. Korfei M, Skwarna S, Henneke I, MacKenzie B, Klymenko O, Saito S, et al. Aberrant expression and activity of histone deacetylases in sporadic idiopathic pulmonary fibrosis. Thorax. 2015;70(11):1022–32.

40. Seet LF, Chu SW, Toh LZ, Teng X, Yam GH, Wong TT. Valproic acid modulates collagen architecture in the postoperative conjunctival scar. J Mol Med (Berl). 2022;100(6):947–61.

41. Costalonga EC, de Freitas LJ, Aragone D, Silva FMO, Noronha IL. Anti-fibrotic effects of valproic acid in experimental peritoneal fibrosis. PLoS One. 2017;12(9):e0184302.

42. Kawaoka K, Doi S, Nakashima A, Yamada K, Ueno T, Doi T, et al. Valproic acid attenuates renal fibrosis through the induction of autophagy. Clin Exp Nephrol. 2017;21(5):771–80.

43. Hellman KM, Kuhn CS, Tu FF, Dillane KE, Shlobin NA, Senapati S, et al. Cine MRI during spontaneous cramps in women with menstrual pain. Am J Obstet Gynecol. 2018;218(5):506 e1-e8.

44. Vigano P, Candiani M, Monno A, Giacomini E, Vercellini P, Somigliana E. Time to redefine endometriosis including its pro-fibrotic nature. Hum Reprod. 2018;33(3):347–52.

45. Guo SW. Fibrogenesis resulting from cyclic bleeding: the holy grail of the natural history of ectopic endometrium. Hum Reprod. 2018;33:353–6.

46. Matsushita Y, Araki K, Omotuyi O, Mukae T, Ueda H. HDAC inhibitors restore C-fibre sensitivity in experimental neuropathic pain model. Br J Pharmacol. 2013;170(5):991–8.

47. Pirapakaran K, Aggarwal A. The use of low-dose sodium valproate in the management of neuropathic pain: illustrative case series. Intern Med J. 2016;46(7):849–52.

48. Audia JE, Campbell RM. Histone modifications and cancer. Cold Spring Harb Perspect Biol. 2016;8(4):a019521.

49. Rajabi N, Galleano I, Madsen AS, Olsen CA. Targeting Sirtuins: substrate specificity and inhibitor design. Prog Mol Biol Transl Sci. 2018;154:25–69.

50. Gurvich N, Tsygankova OM, Meinkoth JL, Klein PS. Histone deacetylase is a target of valproic acid-mediated cellular differentiation. Cancer Res. 2004;64(3):1079–86.

51. Sixto-Lopez Y, Bello M, Correa-Basurto J. Exploring the inhibitory activity of valproic acid against the HDAC family using an MMGBSA approach. J Comput Aided Mol Des. 2020;34(8):857–78.

52. Colon-Diaz M, Baez-Vega P, Garcia M, Ruiz A, Monteiro JB, Fourquet J, et al. HDAC1 and HDAC2 are differentially expressed in endometriosis. Reprod Sci. 2012;19(5):483–92.

53. Felisbino MB, McKinsey TA. Epigenetics in cardiac fibrosis: emphasis on inflammation and fibroblast activation. JACC Basic Transl Sci. 2018;3(5):704–15.

54. Moran-Salvador E, Mann J. Epigenetics and liver fibrosis. Cell Mol Gastroenterol Hepatol. 2017;4(1):125–34.

55. Chen PJ, Huang C, Meng XM, Li J. Epigenetic modifications by histone deacetylases: biological implications and therapeutic potential in liver fibrosis. Biochimie. 2015;116:61–9.

56. Hyndman KA. Histone deacetylases in kidney physiology and acute kidney injury. Semin Nephrol. 2020;40(2):138–47.

57. Rossi L, Battistelli C, de Turris V, Noce V, Zwergel C, Valente S, et al. HDAC1 inhibition by MS-275 in mesothelial cells limits cellular invasion and promotes MMT reversal. Sci Rep. 2018;8(1):8492.

58. Ryu JK, Kim WJ, Choi MJ, Park JM, Song KM, Kwon MH, et al. Inhibition of histone deacetylase 2 mitigates profibrotic TGF-β1 responses in fibroblasts derived from Peyronie's plaque. Asian J Androl. 2013;15(5):640–5.

59. Li M, Zheng Y, Yuan H, Liu Y, Wen X. Effects of dynamic changes in histone acetylation and deacetylase activity on pulmonary fibrosis. Int Immunopharmacol. 2017;52:272–80.

60. Li X, Wu XQ, Xu T, Li XF, Yang Y, Li WX, et al. Role of histone deacetylases(HDACs) in progression and reversal of liver fibrosis. Toxicol Appl Pharmacol. 2016;306:58–68.

61. Lin W, Zhang Q, Liu L, Yin S, Liu Z, Cao W. Klotho restoration via acetylation of peroxisome proliferation-activated receptor γ reduces the progression of chronic kidney disease. Kidney Int. 2017;92(3):669–79.

62. Wang X, Liu J, Zhen J, Zhang C, Wan Q, Liu G, et al. Histone deacetylase 4 selectively contributes to podocyte injury in diabetic nephropathy. Kidney Int. 2014;86(4):712–25.

63. Xiong C, Guan Y, Zhou X, Liu L, Zhuang MA, Zhang W, et al. Selective inhibition of class IIa histone deacetylases alleviates renal fibrosis. FASEB J. 2019;33(7):8249–62.

64. Ke B, Chen Y, Tu W, Ye T, Fang X, Yang L. Inhibition of HDAC6 activity in kidney diseases: a new perspective. Mol Med. 2018;24(1):33.

65. Tao H, Yang JJ, Shi KH, Li J. Epigenetic factors MeCP2 and HDAC6 control α-tubulin acetylation in cardiac fibroblast proliferation and fibrosis. Inflamm Res. 2016;65(5):415–26.

66. Kang DH, Yin GN, Choi MJ, Song KM, Ghatak K, Minh NN, et al. Silencing histone deacetylase 7 alleviates transforming growth factor-β1-induced Profibrotic responses in fibroblasts derived from Peyronie's plaque. World J Mens Health. 2018;36(2):139–46.

67. Choi SY, Kee HJ, Kurz T, Hansen FK, Ryu Y, Kim GR, et al. Class I HDACs specifically regulate E-cadherin expression in human renal epithelial cells. J Cell Mol Med. 2016;20(12):2289–98.

68. Yan D, Liu X, Xu H, Guo SW. Mesothelial cells participate in endometriosis Fibrogenesis through platelet-induced mesothelial-mesenchymal transition. J Clin Endocrinol Metab. 2020;105:e4124–47.

69. Yoon S, Kang G, Eom GH. HDAC inhibitors: therapeutic potential in fibrosis-associated human diseases. Int J Mol Sci. 2019;20(6):1329.

70. Zhang Q, Duan J, Liu X, Guo SW. Platelets drive smooth muscle metaplasia and fibrogenesis in endometriosis through epithelial-mesenchymal transition and fibroblast-to-myofibroblast transdifferentiation. Mol Cell Endocrinol. 2016;428:1–16.

71. Zhang Q, Duan J, Olson M, Fazleabas A, Guo SW. Cellular changes consistent with epithelial-mesenchymal transition and fibroblast-to-Myofibroblast Transdifferentiation in the progression of experimental endometriosis in baboons. Reprod Sci. 2016;23(10):1409–21.

72. Zheng H, Liu X, Guo SW. Corroborating evidence for aberrant expression of histone deacetylase 8 in endometriosis. Reprod Med Biol. 2023;22(1):e12527.

73. Gaetje R, Kotzian S, Herrmann G, Baumann R, Starzinski-Powitz A. Nonmalignant epithelial cells, potentially invasive in human endometriosis, lack the tumor suppressor molecule E-cadherin. Am J Pathol. 1997;150(2):461–7.

74. Xiao W, Chen X, Liu X, Luo L, Ye S, Liu Y, et al. A histone deacetylase inhibitor, suppresses proliferation and epithelial-mesenchymal transition in retinal pigment epithelium cells. J Cell Mol Med. 2014;18(4):646–55.

75. Zhang Y, Zou J, Tolbert E, Zhao TC, Bayliss G, Zhuang S. Identification of histone deacetylase 8 as a novel therapeutic target for renal fibrosis. FASEB J. 2020;34(6):7295–7310.

76. Animals. NRCUCftUotGftCaUoL. Guide for the care and use of laboratory animals. Washington, DC: National Academies Press; 2011.

77. Yan D, Liu X, Guo SW. The establishment of a mouse model of deep endometriosis. Hum Reprod. 2019;34(2):235–47.

78. Liu X, Yan D, Guo SW. Sensory nerve-derived neuropeptides accelerate the development and fibrogenesis of endometriosis. Hum Reprod. 2019;34(3):452–68.

79. Yan D, Liu X, Guo S-W. Neuropeptides substance P and calcitonin gene related peptide accelerate the development and fibrogenesis of endometriosis. Sci Rep. 2019;9(1):2698.

80. Long Q, Liu X, Guo SW. Surgery accelerates the development of endometriosis in mice. Am J Obstet Gynecol. 2016;215(3):320.e1–320.e15.

81. Balasubramanian S, Ramos J, Luo W, Sirisawad M, Verner E, Buggy JJ. A novel histone deacetylase 8 (HDAC8)-specific inhibitor PCI-34051 induces apoptosis in T-cell lymphomas. Leukemia. 2008;22(5):1026–34.

82. Chakrabarti A, Melesina J, Kolbinger FR, Oehme I, Senger J, Witt O, et al. Targeting histone deacetylase 8 as a therapeutic approach to cancer and neurodegenerative diseases. Future Med Chem. 2016;8(13):1609–34.

83. R Core Team A. R: a language and environment for statistical computing. Vienna, Austria: R Foundation for Statistical Computing; 2021.

84. Li Y, Tang CB, Kilian KA. Matrix mechanics influence fibroblast-Myofibroblast transition by directing the localization of histone deacetylase 4. Cell Mol Bioeng. 2017;10(5):405–15.

85. Ding D, Chen Y, Liu X, Jiang Z, Cai X, Guo SW. Diagnosing deep endometriosis using transvaginal Elastosonography. Reprod Sci. 2020;27(7):1411–22.

86. Song Y, Soto J, Li S. Mechanical regulation of histone modifications and cell plasticity. Curr Opin Solid State Mater Sci. 2020;24(6):100872.

87. Uhler C, Shivashankar GV. Regulation of genome organization and gene expression by nuclear mechanotransduction. Nat Rev Mol Cell Biol. 2017;18(12):717–27.

88. Krusche CA, Vloet AJ, Classen-Linke I, von Rango U, Beier HM, Alfer J. Class I histone deacetylase expression in the human cyclic endometrium and endometrial adenocarcinomas. Hum Reprod. 2007;22(11):2956–66.

89. Chen G, Yan Q, Liu L, Wen X, Zeng H, Yin S. Histone deacetylase 3 governs beta-estradiol-ERalpha-involved endometrial tumorigenesis via inhibition of STING transcription. Cancers (Basel). 2022;14(19):4718.

90. Qu H, Li L, Wang TL, Seckin T, Segars J, Shih IM. Epithelial cells in endometriosis and Adenomyosis upregulate STING expression. Reprod Sci. 2020;27(6):1276–84.

91. Mao C, Liu X, Guo S-W. Reduced endometrial expression of histone deacetylase 3 (HDAC3) in women with adenomyosis who complained of heavy menstrual bleeding. Reprod BioMed Online. 2023. doi:h10.1016/j.rmbo.2023.103288

92. Kim TH, Yoo JY, Choi KC, Shin JH, Leach RE, Fazleabas AT, et al. Loss of HDAC3 results in nonreceptive endometrium and female infertility. Sci Transl Med. 2019;11(474):eaaf7533.

93. Huang Q, Liu X, Guo SW. Higher fibrotic content of endometriotic lesions is associated with diminished prostaglandin E2 signaling. Reprod Med Biol. 2022;21(1):e12423.

94. Huang Q, Liu X, Guo SW. Changing prostaglandin E2 (PGE(2)) signaling during lesional progression and exacerbation of endometriosis by inhibition of PGE(2) receptor EP2 and EP4. Reprod Med Biol. 2022;21(1):e12426.

95. Waltregny D, De Leval L, Glenisson W, Ly Tran S, North BJ, Bellahcene A, et al. Expression of histone deacetylase 8, a class I histone deacetylase, is restricted to cells showing smooth muscle differentiation in normal human tissues. Am J Pathol. 2004;165(2):553–64.

96. Waltregny D, Glenisson W, Tran SL, North BJ, Verdin E, Colige A, et al. Histone deacetylase HDAC8 associates with smooth muscle alpha-Actin and is essential for smooth muscle cell contractility. FASEB J. 2005;19(8):966–8.

97. Anglesio MS, Papadopoulos N, Ayhan A, Nazeran TM, Noe M, Horlings HM, et al. Cancer-associated mutations in endometriosis without cancer. N Engl J Med. 2017;376(19):1835–48.

98. Suda K, Nakaoka H, Yoshihara K, Ishiguro T, Tamura R, Mori Y, et al. Clonal expansion and diversification of cancer-associated mutations in endometriosis and Normal endometrium. Cell Rep. 2018;24(7):1777–89.

99. Lac V, Verhoef L, Aguirre-Hernandez R, Nazeran TM, Tessier-Cloutier B, Praetorius T, et al. Iatrogenic endometriosis harbors somatic cancer-driver mutations. Hum Reprod. 2019; 34(1):69–78.

100. Fonseca MAS, Haro M, Wright KN, Lin X, Abbasi F, Sun J, et al. Single-cell transcriptomic analysis of endometriosis. Nat Genet. 2023;55(2):255–67.

101. Bitler BG, Wu S, Park PH, Hai Y, Aird KM, Wang Y, et al. ARID1A-mutated ovarian cancers depend on HDAC6 activity. Nat Cell Biol. 2017;19(8):962–73.

102. Hsieh TH, Hsu CY, Wu CW, Wang SH, Yeh CH, Cheng KH, et al. Vorinostat decrease M2 macrophage polarization through ARID1A(6488delG)/HDAC6/IL-10 signaling pathway in endometriosis-associated ovarian carcinoma. Biomed Pharmacother. 2023;161:114500.

103. Campiani G, Cavella C, Osko JD, Brindisi M, Relitti N, Brogi S, et al. Harnessing the role of HDAC6 in idiopathic pulmonary fibrosis: design, synthesis, structural analysis, and biological evaluation of potent inhibitors. J Med Chem. 2021;64(14):9960–88.

104. Fontana A, Cursaro I, Carullo G, Gemma S, Butini S, Campiani G. A therapeutic perspective of HDAC8 in different diseases: an overview of selective inhibitors. Int J Mol Sci. 2022;23(17):10014.

105. Tosti C, Pinzauti S, Santulli P, Chapron C, Petraglia F. Pathogenetic mechanisms of deep infiltrating endometriosis. Reprod Sci. 2015;22(9):1053–9.

SUPPORTING INFORMATION

Additional supporting information can be found online in the Supporting Information section at the end of this article.